Supporting Information

Boosting Oxygen Evolution Electrocatalysis via CeO$_2$ Engineering on Fe$_2$N nanoparticles for rechargeable Zn-air batteries

Minghui Wang[a], Jianwei Ren[b,*], Hui Wang[a], Xuyun Wang[a], Rongfang Wang[a,*]

[a] College of Chemical Engineering, Qingdao University of Science and Technology, Qingdao, 266042, China

[b] Department of Mechanical Engineering Science, University of Johannesburg, Cnr Kingsway and University Roads, Auckland Park, 2092, Johannesburg, South Africa

*Corresponding author.

E-mail address: jren@uj.ac.za (J. Ren), rfwang@qust.edu.cn (R. Wang)

Electrochemical measurements

All oxygen reduction reaction (ORR) and oxygen evolution reaction (OER) tests were performed in a three-electrode system. The ORR test was carried out in 0.1 M KOH solution, and a catalyst-modified platinum-carbon electrode (GCE), Ag/AgCl electrode and platinum wire were used as working electrode, reference electrode and counter electrode, respectively. The catalyst film was prepared as following: the catalyst is ultrasonically dispersed in a 0.25 wt.% Nafion/isopropanol solution with a volume ratio of 1:0.2. Sequentially, 8 μL of the dispersion droplet was applied to the electrode surface and dried naturally. For comparison purpose, a commercial Pt/C (20

wt.%, Johnson Matthey) catalyst electrode was also prepared in the same manner. The measured data is converted into the corresponding standard reversible hydrogen electrode potential (RHE) by the Nernst equation:

$$E_{RHE} = E_{Ag/AgCl} + 0.059\,pH + 0.197\,V$$.

OER tests were performed in 1.0 M KOH solution. The nickel foam loaded with 3 mg of the as-prepared catalyst was used as working electrode, the carbon rod was used as counter electrode, and Hg/HgO was used as reference electrode, respectively. All potentials are IR corrected. The measured data is also converted into the corresponding standard reversible hydrogen electrode potential by the following formula: $E_{RHE} = E_{Hg/HgO} + 0.059\,pH + 0.098\,V$.

Zinc-air battery (ZAB) test: A Zab cell was assembled with the prepared sample as the cathode, zinc foil as the anode, and a mixture of 6 M KOH and 0.2 M $Zn(CH_3OO)_2$ as the electrolyte, respectively. Typically, 4 mg of catalyst, 3 μL of PTFE and 4 mg of conductive carbon black were added to 350 μL of isopropanol and the mixture was stirred to obtain a uniform slurry. The slurry was dried at 40 °C before rolling into sheets, which were pressed against nickel foam under a pressure of 20 MPa.
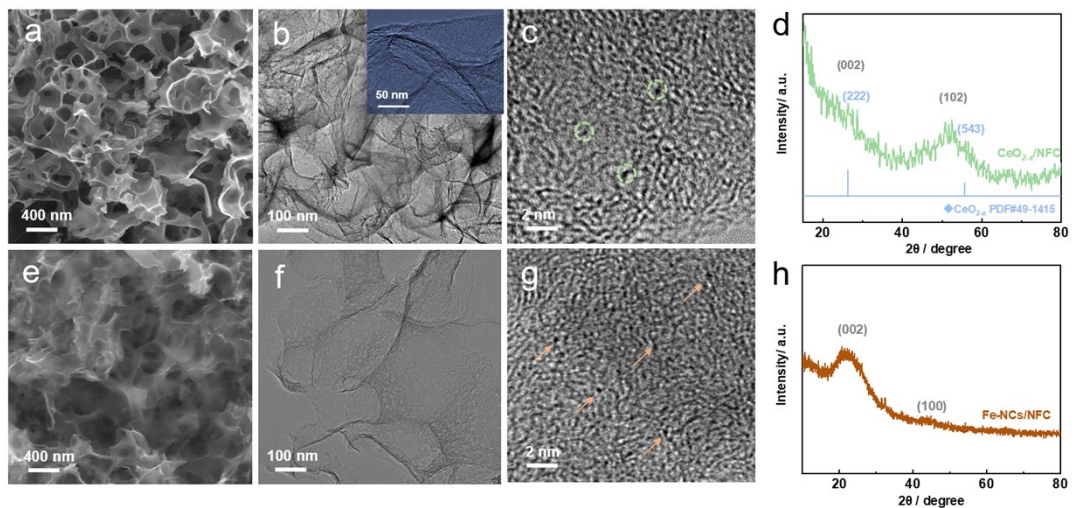
Fig. S1. SEM images of: (a) CeO_{2-x}/NFC and (e) Fe-NCs/NFC samples. TEM images of: (b, f) CeO_{2-x}/NFC and (c, g) Fe-NCs/NFC samples; XRD patterns of: (d) CeO_{2-x}/NFC and (h) Fe-NCs/NFC samples.
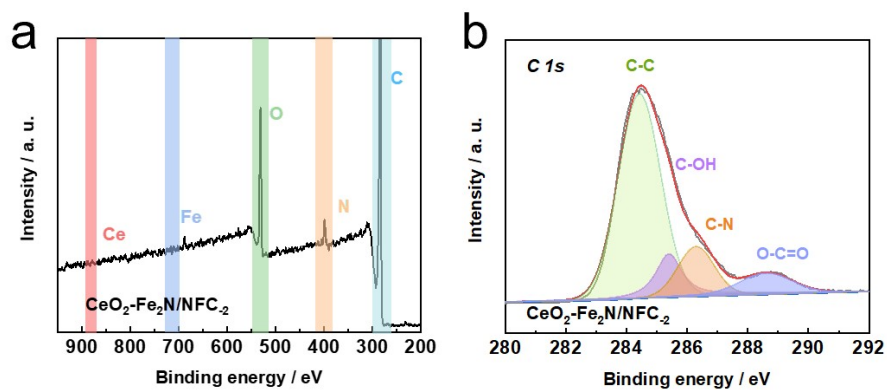

Fig. S2. XPS spectra of CeO_2-Fe_2N/NFC$_{-2}$ sample: (a) Survey spectra and (b) high-resolution C 1s.
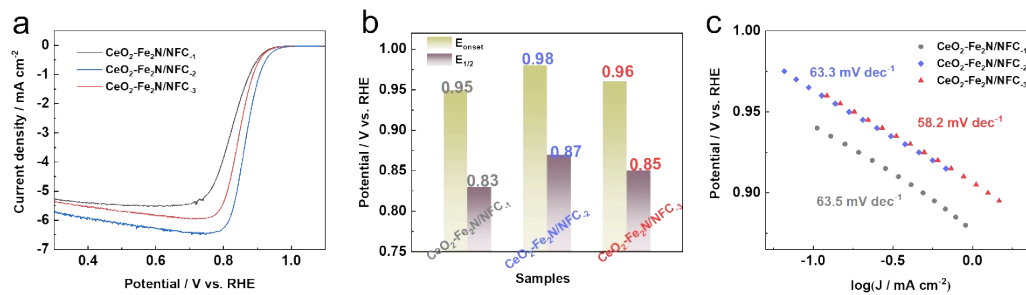
Fig. S3. (a) LSV curves; (b) E_{onset} and $E_{1/2}$; (c) Tafel plots of CeO_2-Fe_2N/NFC$_{-1}$, CeO_2-Fe_2N/NFC$_{-2}$ and CeO_2-Fe_2N/NFC$_{-3}$ samples.
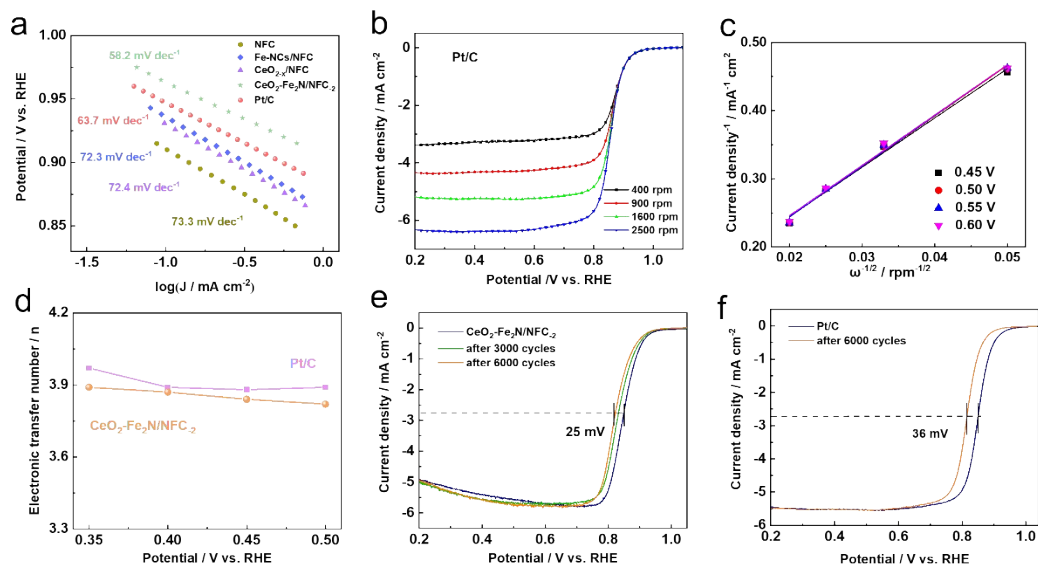
Fig. S4. (a) Tafel plots of NFC, Fe-NCs/NFC, CeO_{2-x}/NFC, CeO_2-Fe_2N/NFC$_{-2}$ and Pt/C samples. (b) The polarization curves at different rotation rates; (c) corresponding K-L plots of Pt/C sample; (d) electronic transfer number of CeO_2-Fe_2N/NFC$_{-2}$ and Pt/C samples. The 1st and 6000th ORR cycles of samples (e) CeO_2-Fe_2N/NFC$_{-2}$ and (f) Pt/C.
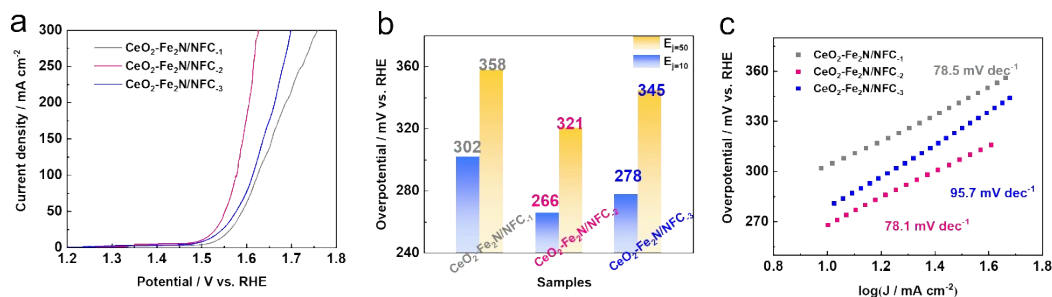
Fig. S5. (a) LSV curves; (b) overpotentials at 50 and 10 mA cm^{-2}; (c) Tafel plots of CeO_2-Fe_2N/NFC$_{-1}$, CeO_2-Fe_2N/NFC$_{-2}$ and CeO_2-Fe_2N/NFC$_{-3}$ samples.
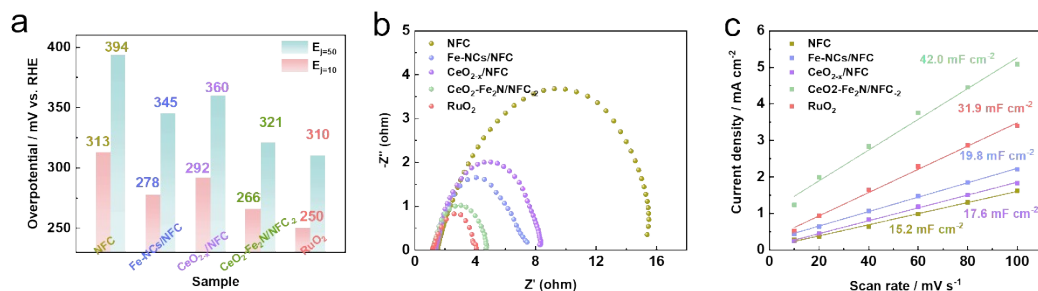

Fig. S6. (a) Overpotentials at 50 and 10 mA cm^{-2}; (b) EIS Nyquist plots at 1.54 V vs.

4

RHE; (c) fitting plots of the current density vs the san rate of five samples ($\Delta j = j_a - j_c$) of NFC, Fe-NCs/NFC, CeO$_{2-x}$/NFC, CeO$_2$-Fe$_2$N/NFC$_{-2}$ and RuO$_2$ samples.
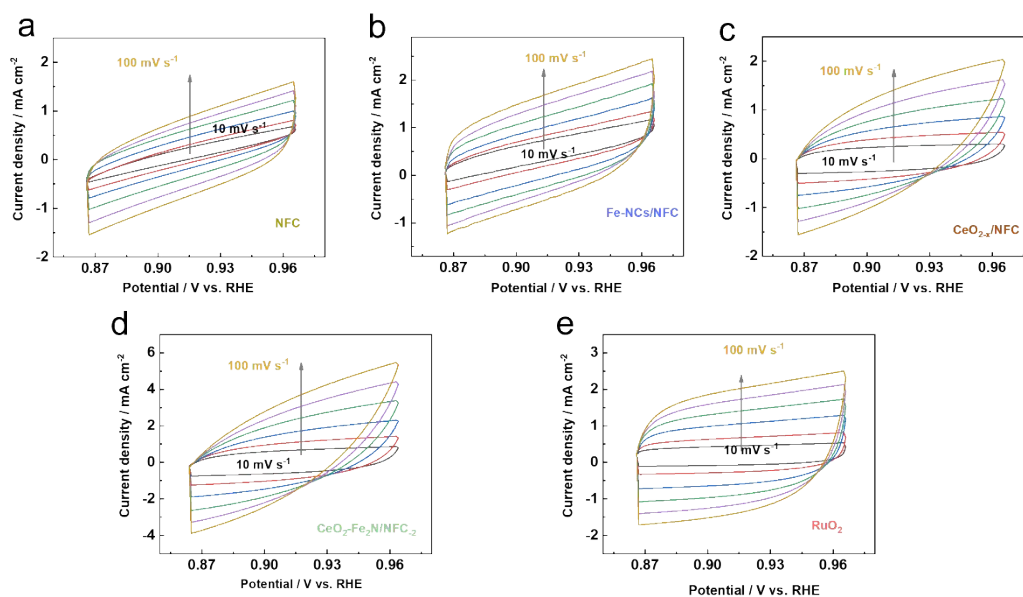

Fig. S7. The electrical double-layer capacitance (C_{dl}) of samples: (a) NFC; (b) Fe-NCs/NFC; (c) CeO$_{2-x}$/NFC; (d) CeO$_2$-Fe$_2$N/NFC$_{-2}$ and (e) RuO$_2$.
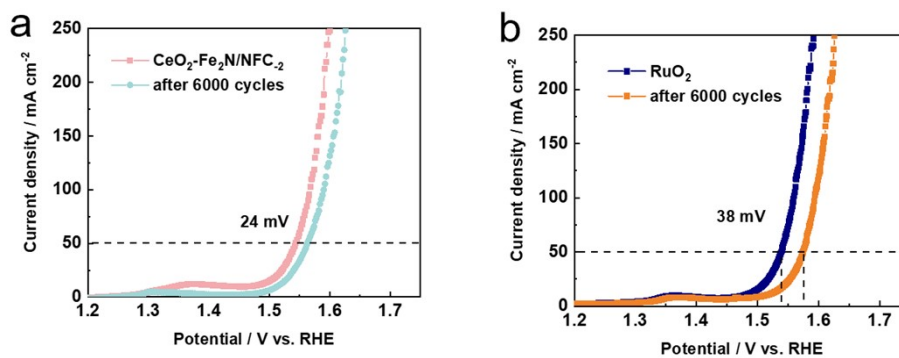
Fig. S8. LSV curves of 1st and 6000th cycles for OER: (a) CeO$_2$-Fe$_2$N/NFC$_{-2}$ sample and (b) RuO$_2$ sample.

Fig. S9. The XRD patterns of the CeO_2-Fe_2N/NFC_{-2} sample: (a) after ORR stability test; and (b) after OER stability test.

Fig. S10. The SEM images of the CeO_2-Fe_2N/NFC_{-2} sample: (a) after ORR stability test; and (b) after OER stability test.
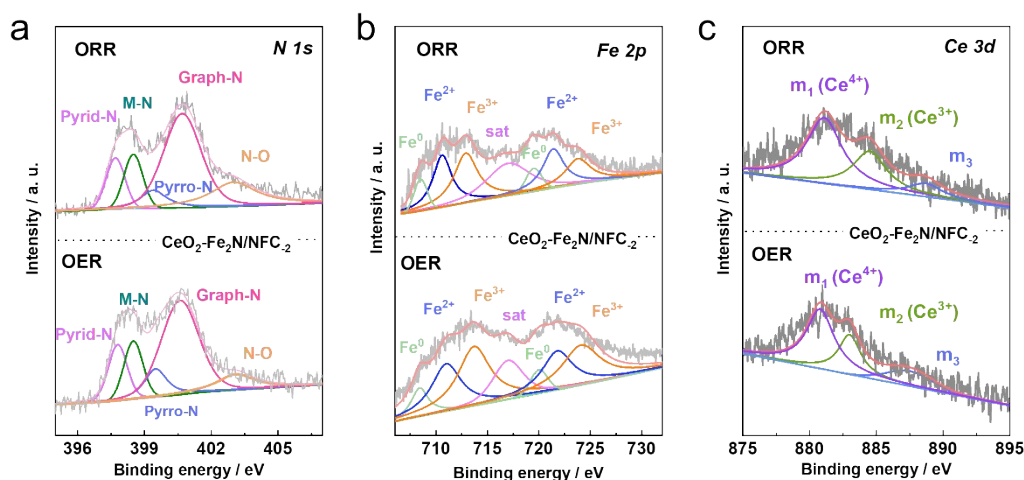
Fig. S11. The high-resolution XPS spectra of the CeO_2-Fe_2N/NFC_{-2} sample after ORR

and OER stability tests: (a) N1s; (b) Fe 2p; and (c) Ce 3d.
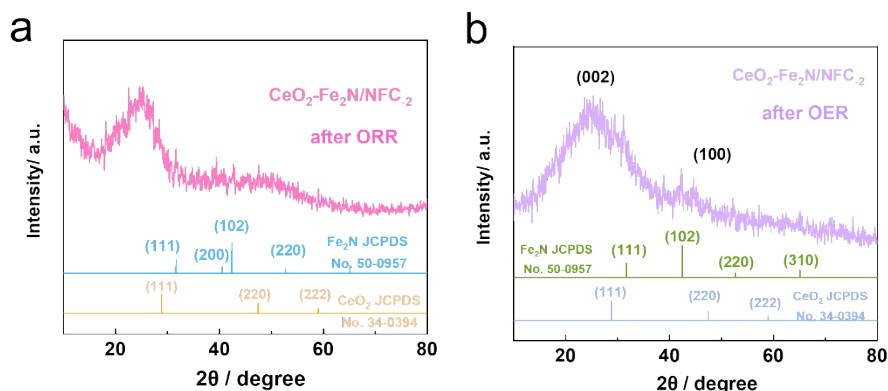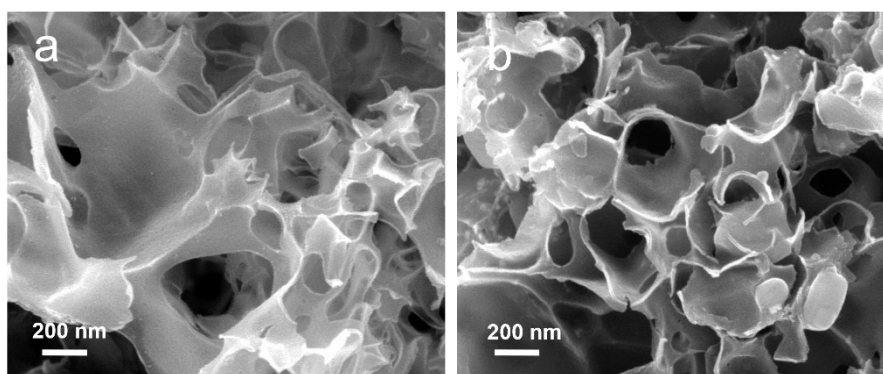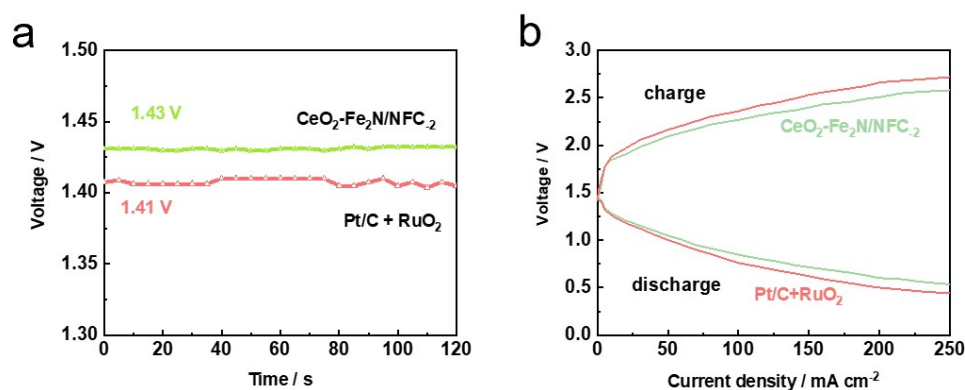

Fig. S12. (a) The open circuit voltages; (b) charge/discharge polarization curves of $CeO_2\text{-}Fe_2N/NFC_{-2}$ and $Pt/C+RuO_2$-based ZAB cells.

Table S1. The atomic percentages (at%) of the samples determined from the XPS analysis.

Sample	C	O	N	Fe	Ce
Fe-NCs/NFC	93.95	3.46	2.26	0.33	0
$CeO_{2\text{-}x}/NFC$	88.07	9.12	2.76	0	0.05
$CeO_2\text{-}Fe_2N/NFC_{-2}$	85.19	11.26	3.11	0.39	0.04

Table S2. Conductivities (S/m) of the prepared samples at different voltages.

Voltages (mV)	Fe-NCs/NFC	$CeO_{2\text{-}x}/NFC$	$CeO_2\text{-}Fe_2N/NFC_{-2}$
0.3	536.2	182	235.9
0.5	188	119	134.6
0.8	74.7	65.9	72.3

Table S3. The ORR/OER performance comparison of CeO_2-Fe_2N/NFC$_{-2}$ sample with various catalysts reported in literature.

Catalysts	ORR	OER	Oxygen electrode activity	References
	$E_{1/2}$ (V vs. RHE)	$E_{j=10\,mA\,cm^{-2}}$ (V vs. RHE)	$\triangle E = E_{j=10\,mA\,cm^{-2}} - E_{1/2}$ (V vs. RHE)	
CeO_2-Fe_2N/NFC$_{-2}$	0.87	1.49	0.62	This work
Co-CeO_2/C	0.75	1.61	0.86	[1]
3Co–LaMOH|O$_V$@NC	0.83	1.56	0.73	[2]
CeO_2@$CoSe_2$-NCs	0.76	1.55	0.79	[3]
CeO_2-FeNC-5	0.90	1.55	0.65	[4]
FeNi@N-CNT/NCS	0.84	1.59	0.75	[5]
FeCo–NC$_{ps}$	0.85	1.61	0.76	[6]
SA-Fe-Nx-MPCS	0.88			[7]
Fe-MNC	0.85	1.53	0.68	[8]
FeNC-CoS_2	0.85	1.61	0.76	[9]
Fe-NSDC	0.84	1.65	0.81	[10]
Ce/Fe-NCNW	0.91			[11]
Fe–Me–Ni	0.84	1.54	0.70	[12]
Mn-RuO_2	0.86	1.50	0.64	[13]

Table S4. Summary of recently reported high-performance rechargeable Zn-air batteries with various bi-functional electrocatalysts.

Catalysts	Peak power density (mW cm^{-2})	charge/discharge voltage gap (V)	References
CeO_2-	133	0.68 @20 mA cm^{-2}	This work

Fe$_2$N/NFC$_{-2}$			
3Co–LaMOH|O$_V$@NC	110	0.98 @5 mA cm^{-2}	2
CeO$_2$@CoSe$_2$-NCs	153	0.86 @5 mA cm^{-2}	3
CeO$_2$-FeNC-5	169	0.83 @10 mA cm^{-2}	4
FeNi@N-CNT/NCS	103	0.73 @10 mA cm^{-2}	5
Fe-MNC	137		8
M-2	124	0.71 @20 mA cm^{-2}	14

References

1   Z. Liu, J. Wan, M. Li, Z. Shi, J. Liu and Y. Tang, *Nanoscale.*, 2022, **14**, 1997-2003.

2   J. Zhang, J. Chen, Y. Luo, Y. Chen, C. Zhang, Y. Luo, Y. Xue, H. Liu, G. Wang and R. Wang, *J. Energy Chem.*, 2021, **60**, 503-511.

3   Y. Huang, Y. Liu, Y. Deng, J. Zhang, B. He, J. Sun, Z. Yang, W. Zhou and L. Zhao, *J. Colloid Interface Sci.*, 2022, **625**, 839-849.

4   Y. Huang, Y. Zhang, J. Hao, Y. Wang, J. Yu, Y. Liu, Z. Tian, T. S. Chan, M. Liu, W. Li and J. Li, *J. Colloid Interface Sci.*, 2022, DOI: 10.1016/j.jcis.2022.09.066, 1067–1076.

5   J.-T. Ren, L. Chen, Y.-S. Wang, W.-W. Tian, L.-J. Gao and Z.-Y. Yuan, *ACS Sustain. Chem. Eng.*, 2019, **8**, 223-237.

6   J. Liu, T. He, Q. Wang, Z. Zhou, Y. Zhang, H. Wu, Q. Li, J. Zheng, Z. Sun, Y. Lei, J. Ma and Y. Zhang, *J. Mater. Chem. A.*, 2019, **7**, 12451-12456.

7   X. Fu, G. Jiang, G. Wen, R. Gao, S. Li, M. Li, J. Zhu, Y. Zheng, Z. Li, Y. Hu, L. Yang, Z. Bai, A. Yu and Z. Chen, *Appl. Catal. B.*, 2021, **293**, 120176-120184.

8   X. Luo, Z. Liu, Y. Ma, Y. Nan, Y. Gu, S. Li, Q. Zhou and J. Mo, *J. Alloys Compd.*, 2021, **888**, 161464-161472.

9   Y. Mi, W. Wang, Y. Hao, Y. Kang, S. Imhanria and Z. Lei, *J. Taiwan Inst. Chem. Eng.*, 2021, **118**, 334-341.

10 J. Zhang, M. Zhang, Y. Zeng, J. Chen, L. Qiu, H. Zhou, C. Sun, Y. Yu, C. Zhu and Z. Zhu, *Small.*, 2019, **15**, 1900307-1900317.

11 J.-C. Li, S. Maurya, Y. S. Kim, T. Li, L. Wang, Q. Shi, D. Liu, S. Feng, Y. Lin and M. Shao, *ACS Catal.*, 2020, **10**, 2452-2458.

12 Y. Tang, Y. Lei, G. Li, T. Fu, Y. Xiang, J. Sha, H. Yang, P. Yu, Y. Si and C. Guo, *J. Mater. Chem. A.*, 2022, **10**, 5305-5316.

13 C. Zhou, X. Chen, S. Liu, Y. Han, H. Meng, Q. Jiang, S. Zhao, F. Wei, J. Sun, T. Tan and R. Zhang, *J. Am. Chem. Soc.*, 2022, **144**, 2694-2704.

14 J. Ding, P. Wang, S. Ji, H. Wang, V. Linkov and R. Wang, *Electrochim. Acta.*, 2019, **296**, 653-661.